

## KB-0118, A novel BET bromodomain inhibitor, suppresses Th17-mediated inflammation in inflammatory bowel disease

Yeo-Jin Jeong<sup>a,b</sup>, Yeon-Su Ok<sup>a</sup>, Gi-Nam Kwon<sup>a</sup>, Min-Young Kim<sup>c</sup>, Jin Hong Chun<sup>c</sup>, Sukmo Kang<sup>c</sup>, Haemi Yang<sup>d</sup>, Minhee Son<sup>d</sup>, In-hyun Lee<sup>d</sup>, Gi-Cheon Kim<sup>a,\*</sup>, Ho-Keun Kwon<sup>a,b,e,f,\*\*,1</sup>

<sup>a</sup> Department of Microbiology and Immunology, Yonsei University College of Medicine, Seoul 03722, Republic of Korea

<sup>b</sup> Graduate School of Medical Science, Brain Korea 21 Project, Yonsei University College of Medicine, Seoul, Republic of Korea

<sup>c</sup> Keyfron Bio Co., Ltd., Cheongju-si, Chungcheongbuk-do 28115, Republic of Korea

<sup>d</sup> Benobio Co., Ltd., Seongnam-si, Gyeonggi-do 13494, Republic of Korea

<sup>e</sup> Institute for Immunology and Immunological Diseases, Yonsei University College of Medicine, Seoul 03722, Republic of Korea

<sup>f</sup> Pohang University of Science and Technology, Pohang 37673, Republic of Korea

### ARTICLE INFO

#### Keywords:

BET Bromodomain inhibitor  
KB-0118  
Inflammatory bowel disease  
T helper 17 cells

### ABSTRACT

Inflammatory bowel disease (IBD) presents complex pathologies and remains challenging to treat, highlighting the urgent need for innovative therapeutics. This study evaluates KB-0118, a novel BET bromodomain inhibitor targeting BRD4, for its immunomodulatory effects in IBD. KB-0118 effectively inhibited pro-inflammatory cytokines, including TNF, IL-1 $\beta$ , and IL-23a, and selectively suppressed Th17 cell differentiation, a critical driver of IBD pathology. In both DSS-induced and T cell-mediated colitis models, KB-0118 significantly reduced disease severity, preserved colon structure, and lowered IL-17 expression. Mechanistic studies suggest KB-0118's modulation of Th17-driven inflammation occurs through epigenetic suppression of BRD4, confirmed by transcriptomic analysis showing downregulation of STAT3 and BRD4 target genes. Compared to standard BET inhibitors like JQ1 and MS402, KB-0118 exhibited enhanced efficacy in restoring immune balance in IBD, positioning it as a promising therapeutic candidate for chronic inflammatory diseases. Further investigation into KB-0118's specificity and long-term effects will be essential to clarify its full clinical potential.

### 1. Introduction

The bromodomain and extraterminal domain (BET) protein family, comprising BRD2, BRD3, BRD4, and BRDT, is essential for mediating interactions with acetylated proteins via acetyl-lysine-binding bromodomains. Among these, BRD4 has emerged as a pivotal epigenetic regulator due to its strong binding to transcriptionally active DNA, where it modulates chromatin dynamics, gene expression, cell cycle progression, and cellular differentiation [1,2]. BRD4's regulatory capacity in these processes has identified it as a key target in oncology, with numerous studies confirming the efficacy of BRD4 inhibitors in various malignancies, such as acute myeloid leukemia, multiple myeloma, and glioblastoma [3,4]. BET inhibitors, particularly those targeting BRD4, have demonstrated therapeutic promise in both preclinical and clinical studies, where they reduce tumor growth and suppress tumor-initiating

cells by modulating MYC and other oncogenic pathways[5]. Beyond oncology, BRD4 has recently been implicated in inflammatory pathways, influencing the production of pro-inflammatory cytokines in innate immune cells, which extends the therapeutic applications of BET inhibitors to inflammatory and autoimmune diseases. Preclinical studies have shown that BRD4 inhibition can reduce inflammation in models of osteoarthritis and rheumatoid arthritis, highlighting its therapeutic relevance in chronic inflammatory conditions [6–8]. Early-phase clinical trials are exploring the efficacy of BET inhibitors in non-cancerous inflammatory conditions. Initial studies show that BET inhibition can reduce inflammation by modulating pro-inflammatory pathways, highlighting its therapeutic potential in autoimmune diseases and fibrosis. Recent investigations demonstrate that BET inhibitors attenuate inflammatory responses in diseases like rheumatoid arthritis and lung fibrosis, supporting their use across a broad range of conditions [9–11].

\* Corresponding author.

\*\* Corresponding author at: Department of Microbiology and Immunology, Yonsei University College of Medicine, Seoul 03722, Republic of Korea.

E-mail addresses: [KIMGCC35@yuhs.ac](mailto:KIMGCC35@yuhs.ac) (G.-C. Kim), [HK@yuhs.ac](mailto:HK@yuhs.ac) (H.-K. Kwon).

<sup>1</sup> These authors have contributed equally to this work and share corresponding authorship.

<https://doi.org/10.1016/j.bioph.2025.117933>

Received 24 December 2024; Received in revised form 8 February 2025; Accepted 18 February 2025

Available online 14 March 2025

0753-3322/© 2025 The Authors. Published by Elsevier Masson SAS. This is an open access article under the CC BY-NC-ND license (<http://creativecommons.org/licenses/by-nc-nd/4.0/>).

Inflammatory Bowel Disease (IBD), a chronic, relapsing inflammatory condition of the gastrointestinal tract, primarily manifests as Crohn's Disease (CD) and Ulcerative Colitis (UC). Its pathogenesis involves complex interactions among genetic susceptibility, environmental triggers, gut microbiota alterations, and immune dysregulation. An aberrant immune response to intestinal antigens, with autoimmune characteristics, underlies IBD pathology, resulting in chronic inflammation and intestinal tissue damage [12]. In IBD, immune homeostasis disruption leads to persistent gut mucosal inflammation, primarily driven by CD4<sup>+</sup> T cells, particularly Th17 cells, which are known for their production of IL-17, an inflammatory cytokine implicated in mucosal immunity. While Th17 cells play a protective role against pathogens at mucosal sites, their dysregulation in IBD has been associated with increased disease severity and progression [12]. Elevated IL-17 levels and Th17 cell activity are commonly observed in the intestinal lesions of IBD patients, linking Th17-driven inflammation directly to disease pathology [13,14].

This understanding has led to increased interest in targeting Th17 signaling pathways as a potential therapeutic approach to re-establish immune balance and reduce inflammation in IBD. Recent studies have demonstrated that BET inhibitors effectively modulate Th17-driven immune responses in IBD by epigenetically regulating BRD4 and STAT3-dependent pro-inflammatory pathways, reducing IL-17 and IL-23 production [15–19]. Additionally, BET inhibition has shown promise in modulating the gut-immune axis, highlighting its potential as an innovative therapeutic strategy for IBD. Here, we introduce a novel iBET inhibitor, KB-0118, with significant efficacy in suppressing Th17 responses in preclinical models of IBD, highlighting its therapeutic potential in restoring immune homeostasis and offering a targeted approach to IBD management.

## 2. Material and methods

### 2.1. Screening of the DNA-encoded chemical library (DEL) using the bromodomains of BRD2, BRD3, and BRD4

A DNA-encoded chemical library (DEL) provided by WuXi AppTec (Shanghai, China) was screened to identify novel bromodomain and extra-terminal domain inhibitors (BETi). Screening utilized the BD1 and BD2 domains of BRD2, BRD3, and BRD4 proteins. The gene segments for BRD2, BRD3, and BRD4 were amplified and cloned into pET28a vectors (Novagen, Northumberland, UK), then transformed into *Escherichia coli* BL21(DE3) cells. Protein expression was induced with 0.2 mM isopropyl β-D-thiogalactopyranoside (IPTG) for 16 h at 18 °C. After induction, bacterial cells were harvested, resuspended in lysis buffer (50 mM Tris, pH 8.2; 300 mM NaCl; 20 mM imidazole), and lysed via sonication. Lysates were centrifuged at 1550 × g for 1 h at 4 °C, and the supernatant was loaded onto a HisTrap HP nickel affinity column (GE Healthcare, Chicago, IL, USA) to isolate the proteins, which were eluted using 500 mM imidazole.

### 2.2. Time-resolved fluorescence resonance energy transfer (TR-FRET) assay

A TR-FRET assay was conducted using kits for BRD2 (BD1 + BD2), BRD3 (BD1 + BD2), and BRD4 (BD1 + BD2) from BPS Bioscience (San Diego, CA, USA). The assay was prepared with a master mix containing 1 × BRD homogeneous assay buffer and diluted BD ligands. Following preparation, 1.5 μL of master mix was added to each well of a microplate, and 5 μL of diluted BRD protein was introduced to initiate reactions, which were incubated at 20–22 °C for 30–60 min. GSH acceptor beads and streptavidin-conjugated donor beads (Perkin Elmer, Waltham, MA, USA) were prepared in 1 × BRD detection buffer, and 10 μL of each was sequentially added to each well with incubation steps. Alpha particle counts were measured using an EnVision 2105 multimode plate reader (Perkin Elmer).

### 2.3. Binding kinetics assay

Binding kinetics were measured using the Sartorius Octet® R2 system (Sartorius, Göttingen, Germany) with streptavidin biosensors loaded with biotinylated BRD2 BD1, BRD2 BD2, BRD3 BD1, BRD4 BD1, and BRD4 BD2 proteins. Sensors were immersed in compound solutions for 10 min, and association (kon) and dissociation (koff) rates were recorded. Control sensors with blank PBST were used for parallel measurements. Competitive binding assays were performed by immersing compound-loaded sensors in protein and compound mixtures.

### 2.4. In vitro Caco-2 DSS-induced model

Caco-2 cells were cultured in Dulbecco's modified Eagle's medium (DMEM, pH 7.4) supplemented with 25 mM glucose, 10 % fetal bovine serum (FBS), 1 % penicillin-streptomycin, and 1 % non-essential amino acids. Cells were plated at 5 × 10<sup>3</sup> cells/well in 96-well plates and grown to confluence. KB-0118 was added at concentrations of 0, 0.01, 0.1, and 1 μM. After 24 h, cells were incubated with 5 % DSS (v/v) for 48 h. Viability was assessed using an MTT assay. All analyses were performed in triplicate.

### 2.5. DSS-induced colitis in mice

#### 2.5.1. Animal care and ethical compliance

All animal procedures were approved by the Institutional Animal Care and Use Committee (IACUC) of Keyfron Bio Co., Ltd. (approval number KA23075). Male C57BL/6 mice (6–8 weeks) obtained from ORIENTBIO Inc. (Republic of Korea) were housed under a 12-h light/dark cycle, with temperatures between 19.0–25.0 °C and humidity at 30.0–70.0 %. Food and water were provided ad libitum.

#### 2.5.2. Induction of colitis and disease activity index (DAI) assessment

Colitis was induced by administering 3 % (w/v) dextran sulfate sodium (DSS, 36,000–50,000 MW; MP Biomedicals, Solon, OH, USA) in drinking water for 7 days, with fresh DSS solution provided daily. Control mice received regular water. Colitis severity was monitored daily by calculating a Disease Activity Index (DAI), based on weight loss, stool consistency, and fecal bleeding scores.

#### 2.5.3. Disease activity index (DAI) assessment

The severity of colitis was assessed using a Disease Activity Index (DAI), which is a composite score based on weight loss, stool consistency, and the presence of fecal blood. The DAI score was calculated by summing these parameters to provide an overall assessment of colitis severity.

	Score 0	Score 1	Score 2	Score 3	Score 4
<b>Weight loss</b>	≤ 1 % of baseline or increase	1–5 % loss	5–10 % loss	10–15 % loss	> 15 % loss
<b>Stool Consistency</b>	Normal stool	-	Loose stool (not adhered)	-	Liquid stool (adhered)
<b>Fecal blood</b>	None	-	Moderate bleeding	-	Gross bleeding

Histological parameters		Description	Score
Mucosa	Epithelial cell	Prolonged epithelial cell or crypt	1
		Destruction of barrier	2
		Ulcer (30 % < loss < 60 %)	3
		Ulcer (loss > 60 %)	4
	Immune cell	mild infiltration	1
moderate infiltration		2	
severe infiltration		3	

(continued on next page)

(continued)

Histological parameters		Description	Score
Sub-mucosa	Immune cell	mild infiltration	1
		moderate infiltration	2
		severe infiltration	3

#### 2.5.4. Tissue collection and histological analysis

At the end of the DSS administration period, mice were euthanized by CO<sub>2</sub> inhalation, and colons were harvested. The colons were photographed for documentation and measured for length. They were then rolled into a swiss roll and fixed in 10% neutral buffered formalin overnight. Fixed tissues were sectioned, processed, and embedded in paraffin. Sections of 4–5 μm thickness were cut and stained with Hematoxylin & Eosin (H&E). The H&E-stained slides were examined under a light microscope (Olympus, Japan). Histological colitis scoring was performed based on epithelial and immune cell damage in both mucosa and sub-mucosa, using predefined criteria. Representative images were captured to document the findings.

#### 2.6. Cell culture

Jurkat cells (ATCC, VA, USA) were cultured at a density of  $5 \times 10^5$  cells/mL in RPMI medium. KB-0118 was administered at concentrations of 1 μM, 5 μM, and 10 μM, with a 5 μM DMSO vehicle control. Six h after treatment, 1 μM PMA/Ionomycin was added to activate T cells. After 6 h of stimulation, samples were harvested and dissolved in 1 mL TRIzol reagent (Invitrogen, MA, USA) and stored at –80 °C. RAW 264.7 cells (ATCC, VA, USA) were seeded at  $1 \times 10^5$  cells/well in RPMI medium 24 h before the experiment. The same drug concentrations and treatment conditions were applied as for Jurkat cells, and 1 μg/mL of LPS (O111:B4, Sigma, MO, USA) was added 6 h post-drug treatment. Samples were collected in 1 mL TRIzol and stored at –80 °C.

#### 2.7. RNA extraction and quantitative real-time PCR

Total RNA was isolated from cultured cells using TRIzol reagent (Invitrogen, MA, USA) following the manufacturer's protocol. After lysis, 200 μL of chloroform was added, shaken, and incubated at room temperature for 5 min. The samples were centrifuged at 14,000 rpm for 10 min, and the aqueous phase was removed and mixed with an equal volume of isopropanol. After centrifugation, the RNA pellet was washed with 75% ethanol, air-dried, and resuspended in 20 μL DEPC-treated water. RNA (1 μg) was reverse transcribed using a cDNA synthesis kit (Takara, Japan). Quantitative PCR was performed on a QuantStudio 3 Real-Time PCR System (Thermo Fisher, MA, USA) using PowerUp SYBR Green master mix. The PCR conditions were 40 cycles of 95 °C for 30 sec and 60 °C for 30 s. Gene expression was normalized to *Hprt1*, and relative quantification was calculated using the  $2^{-\Delta\Delta Ct}$  method. Data were analyzed using  $2^{-\Delta\Delta Ct}$  values in GraphPad Prism 10. Statistical significance was assessed by one-way ANOVA and dunnett's multiple t-tests. Heatmaps of Log<sub>2</sub>-transformed  $2^{-\Delta\Delta Ct}$  values were generated using the heatmap package in R.

#### 2.8. CD4<sup>+</sup> naive T cell purification and In Vitro lymphocyte proliferation assay

CD4<sup>+</sup> T cells were enriched using the EasySep Mouse CD4<sup>+</sup> T Cell Isolation Kit (STEMCELL Technologies, Canada). Cells were sorted as DAPI-CD4<sup>+</sup>CD62L<sup>+</sup>CD44<sup>-</sup> naive T cells on a MA900 Cell Sorter (SONY, Japan). CTV-labeled T cells were resuspended at  $2 \times 10^6$  cells/mL in T-cell culture media and stimulated with 1 μg/mL plate-bound anti-CD3 and 2 μg/mL anti-CD28 for 5 days before antibody staining and flow cytometry analysis on a BD Celesta (BD Biosciences, CA, USA). CTV proliferation analysis was conducted using FlowJo software.

#### 2.9. CD4<sup>+</sup> T cell purification, differentiation, and flow cytometric analysis

CD4<sup>+</sup> T cells were purified from the lymph nodes and spleens of 8- to 10-week-old mice using magnetic beads (Miltenyi Biotec, Germany). For Th differentiation, cells ( $1 \times 10^5$ /mL) were stimulated with 1 μg/mL anti-CD3 and 2 μg/mL anti-CD28 in the following conditions:

- Th1: 10 ng/mL IL-12 and 10 μg/mL anti-IL-4.
- Th2: 10 ng/mL IL-4, 10 μg/mL anti-IFN-γ, and 10 μg/mL anti-IL-12.
- Th17: 20 ng/mL IL-6, 0.5 ng/mL TGF-β, 20 ng/mL IL-1β, 10 μg/mL anti-IL-4, and 10 μg/mL anti-IL-12.
- Treg: 1.25 ng/mL TGF-β and 10 μg/mL anti-IL-4 and anti-IL-12.

All conditions were supplemented with 100 U/mL recombinant human IL-2, except for Th17. After differentiation, cells were stained with specific antibodies for T-bet, GATA3, RORγt, Foxp3, IFN-γ, IL-4, and IL-17A. Data were acquired on an ID7000 (SONY, Japan) and analyzed with FlowJo software.

#### 2.10. T cell transfer model of chronic colitis

CD4<sup>+</sup> T cells were isolated using the EasySep Mouse CD4<sup>+</sup> T Cell Isolation Kit, and naive CD4<sup>+</sup>CD45RB<sup>high</sup> T cells were sorted as DAPI<sup>-</sup>CD4<sup>+</sup>CD62L<sup>+</sup>CD44<sup>-</sup>CD45RB<sup>high</sup> on a MA900 Cell Sorter. CD4<sup>+</sup>CD45RB<sup>high</sup> T cells from C57BL/6 mice were injected intravenously into Rag1 KO recipients ( $1 \times 10^6$  cells per mouse in 100 μL PBS). After 2 weeks, mice were treated daily by oral gavage with either 9.97 mg/mL KB-0118 in 0.5% CMC solution, 125 μL per mouse, or with a vehicle-only control. The MS402 group received 10 mg/kg MS402 in a 10% DMSO, 40% PEG400, 5% Tween-80, and 45% PBS solution, administered intraperitoneally every other day. Mice were monitored for clinical colitis signs and DAI score every three days. Eight weeks post-T cell transfer, mice were sacrificed, and colons were collected for analysis.

#### 2.11. IL-17A immunohistochemistry

Tissue sections were deparaffinized with xylene and rehydrated through a graded series of ethanol. Antigen retrieval was performed by heating the sections in sodium citrate buffer (pH 6.0) for 20 min. Endogenous peroxidase activity was blocked using 3% hydrogen peroxide. The anti-IL-17A antibody (ab79056, Abcam, UK) was diluted at 1:200 and incubated at room temperature for 1 hour. After washing with PBS, the sections were incubated with the secondary antibody, Goat Anti-Rabbit IgG-HRP (ab6721, Abcam, UK), at room temperature for 30 min. The signal was developed using DAB (K3468, Dako, Denmark), and the sections were counterstained with hematoxylin, dehydrated, and mounted for analysis. The IL-17A positivity was quantified by calculating the Integrated Density (IntDen)/Total Area. Tissue slides were stained with IL-17A, and a pathologist selected relevant areas for analysis where staining intensity could be accurately assessed. The calculation was performed using the following formula:

$$\text{Integrated Density (IntDen)} = \text{Area} \times \text{Mean Gray Value}^{**}$$

\*Area: The selected region of interest (ROI) determined by the pathologist.

\*\*Mean Gray Value: The average intensity of the pixels within the selected ROI, representing the staining intensity

#### 2.12. Transcriptome analysis

Colon tissue samples were collected from T cell transfer mice, and total RNA was extracted using the Qiagen RNA extraction kit according to the manufacturer's protocol. Bulk RNA sequencing libraries were prepared with the SureSelectXT RNA Direct Library Preparation Kit (Agilent Technologies, CA, USA) and SureSelect XT RNA Direct Protocol,

then sequenced on an Illumina platform to generate paired-end reads with a read length of 101 bp. Raw sequencing reads were pre-processed using Trimmomatic [20] to remove adapters and low-quality bases. The resulting high-quality reads were aligned to the *Mus musculus* genome (mm10) using HISAT2 [21]. Aligned sequencing reads were processed to generate count data using StringTie [22]. Count data were normalized and filtered for  $\text{rowsum} \geq 10$  using DESeq2 package of R software (version 4.3.2), after which differential expression analysis was performed. Genes were considered differentially expressed if  $|\log_2\text{Fold-change}| > 1$ ,  $\text{padj} < 0.05$ .

### 2.13. Statistical and functional analysis

A count of differentially expressed genes (DEGs) between the control (C), vehicle-treated (V), and KB-0118-treated (KB-0118) groups was normalized on a raw scale, and a heatmap was generated using pheatmap (version 1.0.12), with hierarchical clustering of the rows performed based on Euclidean distance. Principal component analysis (PCA) was performed using factextra (version 1.0.7) for scaling and dimensionality reduction and ggbiplot (version 0.55) for visualization. Additionally, volcano plots were generated to display DEGs in KB-0118 compared to V, with ggplot (version 3.5.0). These DEGs were subsequently analyzed for Gene Ontology (GO) enrichment analysis using the Metascape.

#### 2.13.1. Disease signature analysis

Disease associated signature profiling was performed using DEGs from each database, with statistical analysis conducted via chi-square tests. The IBD signature database included 834 DEGs derived from the combined comparisons of CD vs. healthy and UC vs. healthy datasets [23]. The SLE signature database contained 1116 DEGs from SLE vs. healthy [24], and the RA signature database comprised 160 DEGs from RA vs. healthy [25].

#### 2.13.2. Transcription factor enrichment analysis

Transcription factor enrichment analysis was performed on

significantly up- and downregulated genes using the ChEA 2022 dataset through the Enrichr tool (<https://maayanlab.cloud/Enrichr/>).

### 2.14. Statistical analysis

All data were analyzed using SAS software (Version 9.3, SAS Institute Inc., USA). Variance homogeneity was tested using either the Folded-F test or Bartlett's test. Depending on the homogeneity results, Student's *t*-test, Aspin-Welch's *t*-test, one-way ANOVA followed by Dunnett's *t*-test, or Kruskal-Wallis test followed by Steel's test were applied. A *p*-value of less than 0.05 was considered statistically significant.

## 3. Results

### 3.1. Identification of KB-0118 as a selective BET bromodomain inhibitor

Through high-throughput DNA-encoded library (DEL) screening provided by WuXi AppTec, KB-0118 was identified as a promising BET bromodomain inhibitor (Fig. 1A, B). KB-0118 demonstrated selective binding to BRD2 and BRD4 over BRD3, as shown in TR-FRET assays, with notable binding affinity to the BD1 and BD2 domains of BRD2 and BRD4 (Fig. 1C). Binding kinetics analysis further confirmed this specificity, with dissociation constants ( $K_d$ ) of  $36.7 \mu\text{M}$  for BRD2 BD1 and  $47.4 \mu\text{M}$  for BRD4 BD1, highlighting KB-0118's preference for these domains (Fig. 1D). This selectivity suggests that KB-0118 could serve as a targeted therapeutic agent by modulating BRD2 and BRD4-related inflammatory and oncogenic pathways.

### 3.2. Anti-inflammatory effects of KB-0118 in T cells and macrophages

To evaluate the anti-inflammatory potential of KB-0118, we conducted *in vitro* assays using Jurkat T cells and RAW 264.7 macrophages. As illustrated in Fig. 2A, cells were pre-treated with KB-0118 at low (L), medium (M), and high (H) concentrations, followed by stimulation with PMA/ionomycin (Jurkat) or LPS (RAW 264.7) for 6 h. RNA was extracted for quantitative PCR analysis. In Jurkat cells, KB-0118

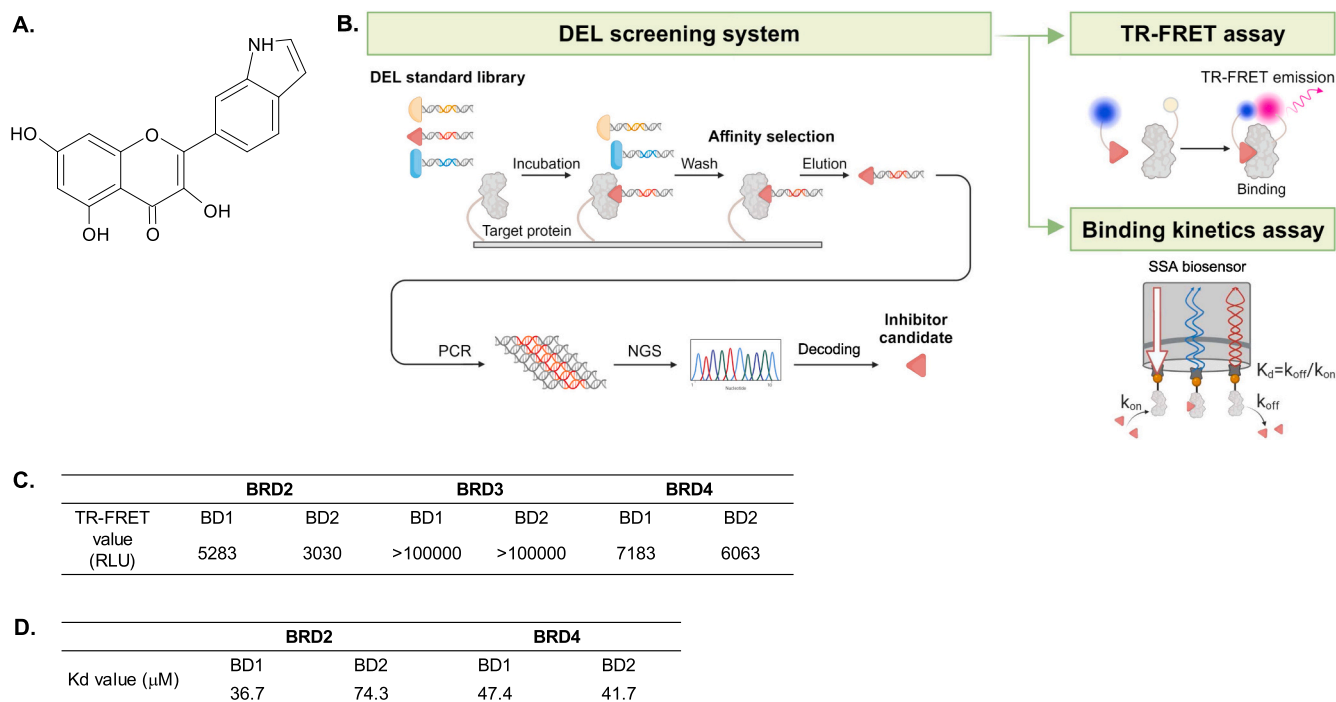


**Fig. 1.** Characterization of KB-0118 as a BET Inhibitor. (A) Chemical structure of KB-0118. (B) Summary of the selection process for KB-0118 as a BET inhibitor, utilizing the DEL screening system followed by TR-FRET and binding kinetics assays. (C) TR-FRET values demonstrating the affinity of KB-0118. (D) Dissociation constant ( $K_d$ ) values from TR-FRET and binding kinetics assays, confirming the binding efficiency of KB-0118.

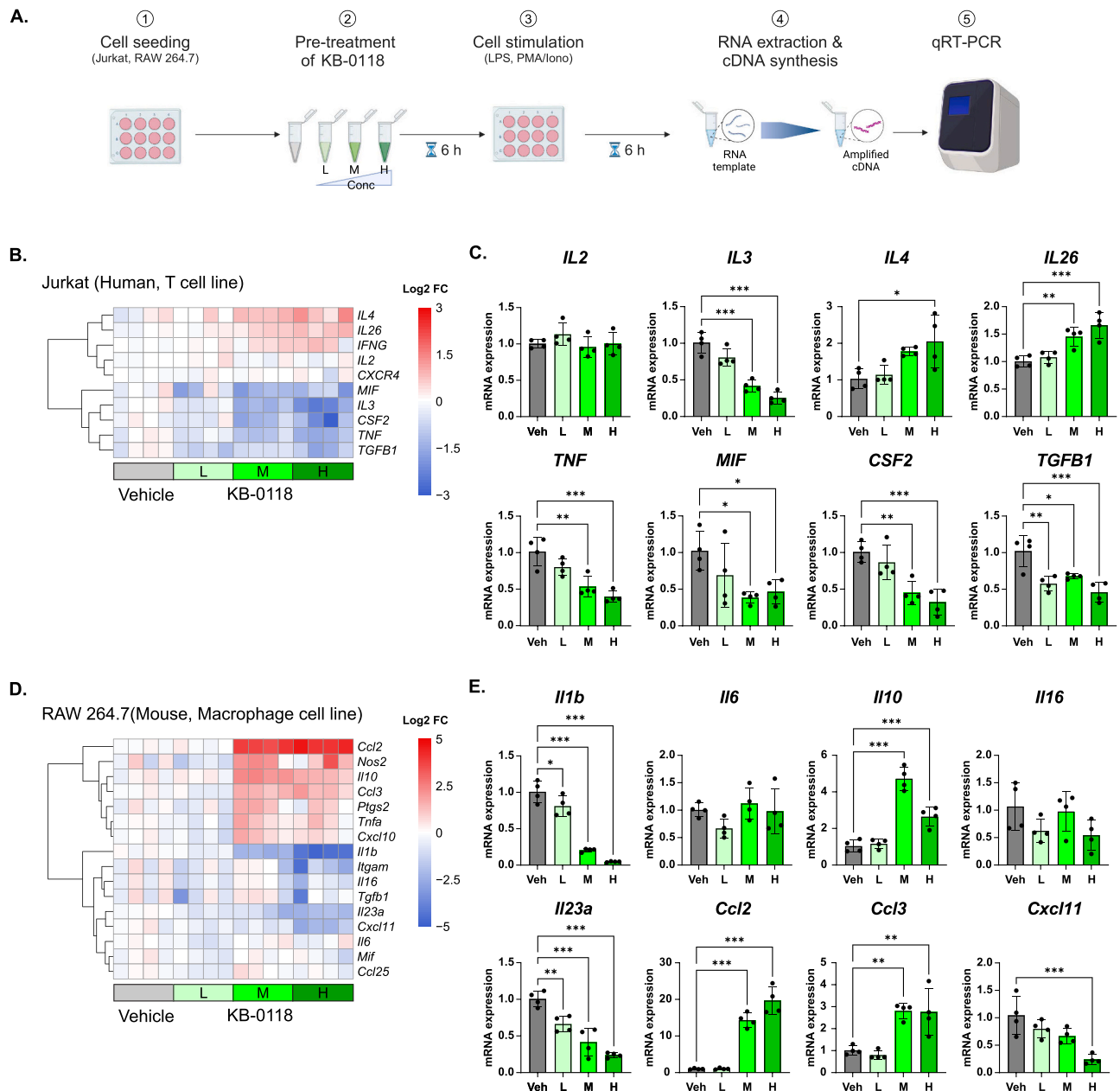


**Fig. 2.** *In Vitro* Efficacy of KB-0118 in T and Macrophage Cell Lines. (A) Schematic representation of the *in vitro* experimental setup. (B) Heatmap illustrating the log<sub>2</sub> fold changes in cytokine expression in Jurkat cells across three KB-0118 treatment concentrations (L: 1 μM, M: 5 μM, H: 10 μM) compared to the vehicle control (5 μM DMSO). (C) Quantification of cytokine expression in Jurkat cells via quantitative RT-PCR, with *HPRT* as a loading control (n = 3 independent experiments). (D, E) Effects of KB-0118 on cytokine expression in Raw264.7 cells. Data are presented as mean ± SD, analyzed by one-way ANOVA with dunnett's multiple comparison test. \*p < 0.05; \*\*p < 0.01; \*\*\*p < 0.005; ns, not significant.

treatment significantly downregulated pro-inflammatory cytokines, particularly *TNF*, *MIF*, and *CSF2*, as shown in the heatmap and individual plots (Fig. 2B and C). These reductions were statistically significant at medium (M) and high (H) doses. Notably, *IL-3* expression decreased, potentially modulating inflammation, as *IL-3* has a detrimental effect during severe colitis by amplifying intestinal inflammation [26]. In RAW 264.7 cells, KB-0118 reduced the expression of *IL-1β*, *IL-6*, *IL-23a*, and chemokines like *Cxcl11*, as depicted in Fig. 2D and E. The suppression of *IL-23a*, which is part of a therapeutic target in IBD, underscores KB-0118's relevance in inflammation control. Additionally, KB-0118 increased the anti-inflammatory cytokine *IL-10*, indicating a potential shift towards an anti-inflammatory profile. Overall, KB-0118 demonstrated a capacity to modulate the cytokine environment, reducing key pro-inflammatory cytokines and enhancing *IL-10*

production, which may contribute to immune homeostasis and reduced inflammatory pathology in IBD.

### 3.3. KB-0118 inhibits T cell proliferation and selectively suppresses *Th17* differentiation while promoting *Th2* polarization

To examine the impact of KB-0118 on T cell proliferation and differentiation, CD4<sup>+</sup> naive T cells were labeled with CellTrace Violet (CTV) and stimulated with anti-CD3 and anti-CD28. CTV dilution, measured by flow cytometry, provided an assessment of cell proliferation. Treatment with KB-0118 significantly reduced T cell proliferation compared to the vehicle-treated group, as evidenced by decreased division, proliferation, expansion, and replication indices (Fig. 3 A). These results indicate a strong inhibitory effect of KB-0118 on T cell

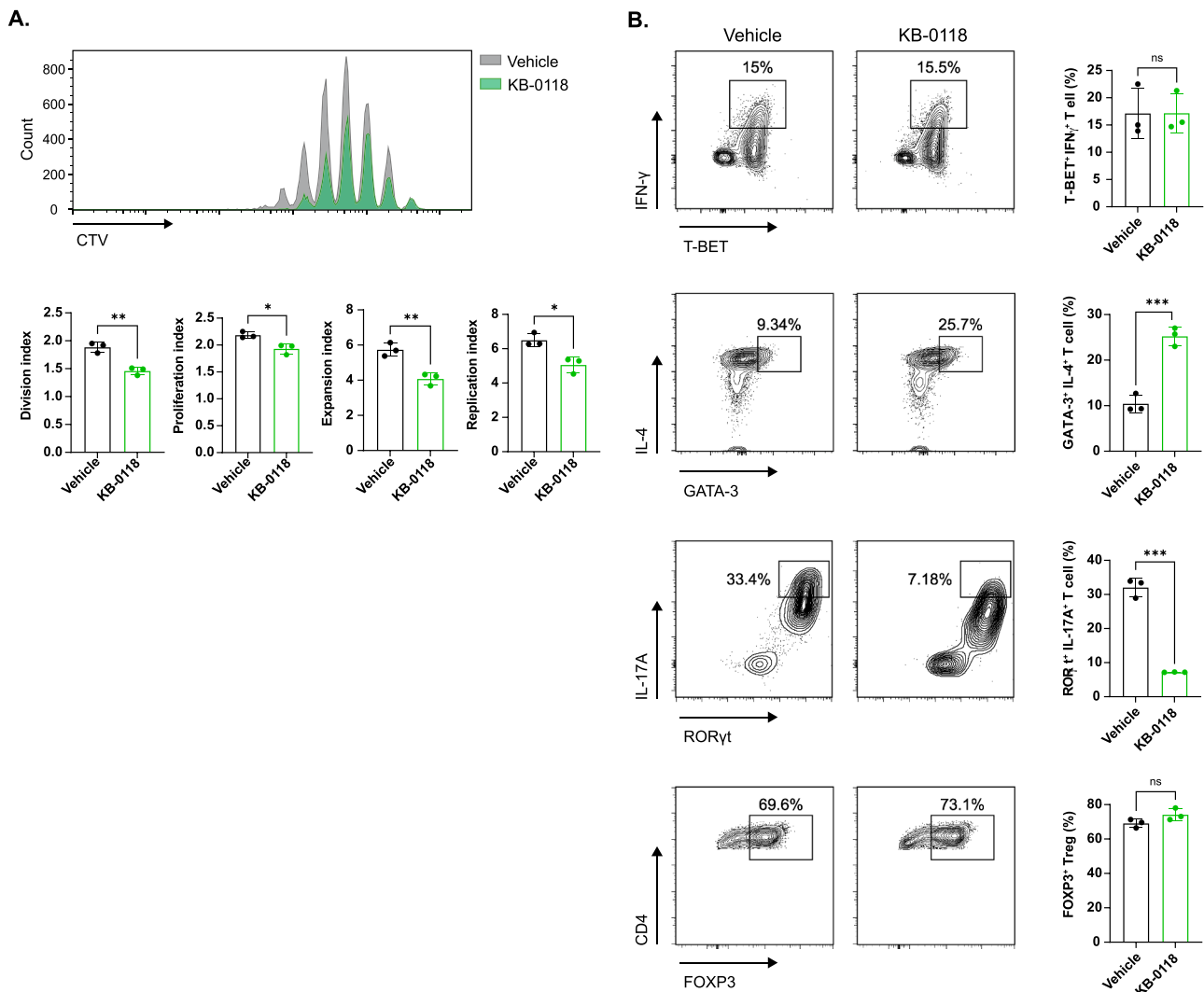


**Fig. 3.** *In vitro* proliferation and differentiation of T Cells in response to KB-0118. (A) Mouse CD4<sup>+</sup> T cells were labeled using cell trace violet (CTV) and activated *in vitro* for 5 days under 5  $\mu$ M KB-0118 and vehicle. Flowjo proliferation analysis histograms for cell division, proliferation, expansion and replication index. (B) Differentiation profiles of CD4<sup>+</sup> T cells were analyzed by flow cytometry, evaluating the expression of key transcription factors and cytokines associated with Th1 (T-bet/IFN- $\gamma$ ), Th2 (GATA-3/IL-4), Th17 (ROR $\gamma$ t/IL-17A), and regulatory T cell (Foxp3) subsets under 5  $\mu$ M KB-0118 and vehicle. Statistical differences were determined by a two-tailed unpaired Student's *t*-test (A, B). \**p* < 0.05, \*\**p* < 0.01, \*\*\**p* < 0.001, not significant (ns) *p*  $\geq$  0.05. Error bars indicate  $\pm$  standard deviation.

proliferation. To further evaluate the influence of KB-0118 on T cell differentiation, we assessed the expression of transcription factors and cytokines associated with different T helper cell subsets [27]. Flow cytometric analysis revealed that KB-0118 selectively affected certain T cell populations. Notably, KB-0118 significantly reduced the proportion of Th17 cells (ROR $\gamma$ t<sup>+</sup> IL-17A<sup>+</sup>), indicating inhibition of Th17 differentiation. Given the role of Th17 cells in promoting inflammation, this finding highlights KB-0118's potential to suppress pro-inflammatory T cell responses. In contrast, KB-0118 increased the proportion of Th2 cells (GATA-3<sup>+</sup> IL-4<sup>+</sup>), suggesting a shift toward an anti-inflammatory Th2 profile. Interestingly, KB-0118 had minimal effect on Th1 (T-BET<sup>+</sup> IFN- $\gamma$ <sup>+</sup>) and regulatory T cells (FOXP3<sup>+</sup>), as their populations remained comparable to those in the vehicle-treated group (Fig. 3B). This selective modulation suggests that KB-0118 can suppress specific pro-inflammatory responses without broadly dampening all T cell activity. Overall, these results suggest that KB-0118 exerts both a broad inhibitory effect on T cell proliferation and a targeted action on T cell differentiation, selectively reducing pro-inflammatory Th17 cells and promoting Th2 differentiation. This unique profile underscores the potential of KB-0118 as a therapeutic agent for controlling excessive immune activation in chronic inflammatory diseases like IBD.

#### 3.4. Therapeutic efficacy of KB-0118 in DSS-induced colitis model

Prior to evaluating KB-0118's therapeutic efficacy in colitis, an *in vivo* toxicity assessment confirmed its safety. Male and female C57BL/6 mice treated with KB-0118 at doses of 50, 100, and 250 mg/kg for 14 days showed no significant weight changes (Figure S1A, B). Hematology and blood chemistry analyses (Table 1, Table 2) revealed minor, non-toxic variations within normal ranges, while histopathology (Table 3) showed minimal tissue findings, confirming KB-0118's tolerability for further studies. Following this toxicity assessment, we proceeded to evaluate KB-0118's therapeutic efficacy in colitis. Male C57BL/6 mice were administered 3% DSS in drinking water for 7 days, with simultaneous treatment of KB-0118 or the reference BET inhibitor JQ1 (Fig. 4A). DSS treatment induced significant weight loss in mice, indicative of colitis development (Fig. 4B). KB-0118 provided a slight, non-significant reduction in weight loss compared to DSS-only mice, suggesting a mild effect on weight maintenance. The Disease Activity Index (DAI), combining weight loss, stool consistency, and fecal bleeding, was elevated in DSS-treated mice, with a modest but non-significant decrease observed in the KB-0118-treated group (Fig. 4C). However, KB-0118 had a significant protective effect on colon length,

**Table 1**

Hematology values for male and female mice administered KB-0118 by oral gavage for 14 days. Although some statistically significant changes were observed, all values remained within the normal reference range for background data, and thus were not considered indicative of toxicity.

Parameters measured	Hematology values (mean ± standard deviation). Treatment doses are in mg/kg bw/day							
	Males (n = 5 per group)				Females (n = 5 per group)			
	Vehicle control	KB-0118 50	100	250	Vehicle control	KB-0118 50	100	250
RBC (×10 <sup>6</sup> /μL)	9.7 ± 0.2	9.9 ± 0.2	9.8 ± 0.4	9.7 ± 0.3	9.4 ± 0.5	10.1 ± 0.2	10.0 ± 0.2	10.2 ± 0.1
HGB (g/dL)	14.3 ± 0.2	14.7 ± 0.4	14.8 ± 0.6	14.7 ± 0.5	14.2 ± 0.8	15.2 ± .3	15.2 ± 0.3	15.1 ± .3
HCT (%)	45.4 ± 0.8	46.9 ± 1.1	46.5 ± 2.0	46.1 ± 1.2	44.2 ± 2.4	47.7 ± 0.4	47.5 ± 1.1	47.8 ± 0.8
MCV (fL)	46.8 ± 0.1	47.4 ± 0.4	47.3 ± 0.6	47.4 ± 0.6	47.1 ± 0.5	47.1 ± 0.5	47.5 ± 0.6	47.1 ± 0.3
MHC (pg)	14.7 ± 0.1	14.8 ± 0.1	15.0 ± 0.1*	15.1 ± 0.1**	15.1 ± 0.2	15.0 ± 0.1	15.2 ± 0.2	14.8 ± 0.1
MCHC (g/dL)	31.4 ± 0.3	31.4 ± 0.4	31.8 ± 0.3	31.8 ± 0.3	32.0 ± 0.5	31.8 ± 0.4	32.0 ± 0.4	31.5 ± 0.3
PLT (×10 <sup>3</sup> /μL)	1368.8 ± 31.4	1410.4 ± 113.1	1392.8 ± 155.4	1269.8 ± 229.9	999.4 ± 145.2	1027.8 ± 170.0	1101.0 ± 69.2	1134.6 ± 50.3
Reti (%)	4.3 ± 0.2	4.3 ± 0.1	4.3 ± 0.2	4.0 ± 0.6	4.0 ± 0.5	3.8 ± 0.3	1.4 ± 0.5	3.7 ± 0.3
WBC (×10 <sup>3</sup> /μL)	5.4 ± 1.4	4.3 ± 1.0	5.0 ± 0.7	4.0 ± 1.6	4.9 ± 1.3	4.7 ± 1.5	6.4 ± 0.8	5.2 ± 1.7
Neu (%)	10.5 ± 1.3	7.4 ± 1.8	7.8 ± 1.1	12.5 ± 12.1	7.5 ± 2.3	7.7 ± 1.6	6.2 ± 1.3	7.1 ± 1.4
Lyn (%)	84.2 ± 2.1	88.7 ± 1.8	88.1 ± 1.7	82.4 ± 11.3	83.3 ± 5.6	87.3 ± 2.6	89.1 ± 1.7	88.7 ± 1.3
Mono (%)	3.2 ± 0.9	2.2 ± 0.2*	2.5 ± 0.6	2.8 ± 0.3	5.1 ± 2.1	2.9 ± 0.6	3.1 ± 0.4	3.0 ± 0.4
Eos (%)	2.1 ± 0.3	1.7 ± 0.3	1.4 ± 0.5	2.2 ± 3.0	3.9 ± 2.1	2.1 ± 1.0	1.6 ± 0.3	1.2 ± 0.4 <sup>#</sup>
Baso (%)	0.0 ± 0.1	0.0 ± 0.0	0.1 ± 0.1	0.0 ± 0.1	0.1 ± 0.1	0.1 ± 0.1	0.1 ± 0.1	0.1 ± 0.1

**Table 2**

Blood chemistry values for male and female mice administered KB-0118 by oral gavage for 14 days. Although some statistically significant changes were observed, these changes were either not dose-dependent or within the normal reference range for background data, and thus were not considered indicative of toxicity.

Parameters measured	Hematology values (mean ± standard deviation). Treatment doses are in mg/kg bw/day							
	Males (n = 5 per group)				Females (n = 5 per group)			
	Vehicle control	KB-0118 50	100	250	Vehicle control	KB-0118 50	100	250
ALT (U/L)	25.4 ± 3.7	25.8 ± 2.0	24.3 ± 3.5	27.8 ± 5.7	21.7 ± 0.9	22.6 ± 6.2	20.2 ± 3.7	21.6 ± 2.2
AST (U/L)	35.9 ± 3.7	37.5 ± 2.7	34.5 ± 1.3	43.1 ± 13.3	38.5 ± 2.0	42.8 ± 7.6	37.4 ± 1.9	39.4 ± 2.2
ALT (U/L)	479.9 ± 16.7	493.9 ± 61.2	504.7 ± 24.8	508.0 ± 124.9	730.9 ± 53.3	714.1 ± 69.2	787.7 ± 53.6	807.4 ± 73.4
Glu (mg/dL)	192.8 ± 13.3	217.8 ± 21.0	216.8 ± 8.5	197.6 ± 32.2	208.2 ± 22.2	213.2 ± 16.7	214.4 ± 31.4	218.6 ± 21.5
BUN (mg/dL)	26.7 ± 2.1	22.4 ± 1.6	20.7 ± 1.7*	22.6 ± 2.9**	26.0 ± 3.4	21.9 ± 2.3	21.6 ± 1.5	25.3 ± 8.1
Crea (mg/dL)	0.3 ± 0.0	0.3 ± 0.0	0.3 ± 0.0	0.3 ± 0.0	0.3 ± 0.0	0.3 ± 0.0	0.3 ± 0.0	0.3 ± 0.0
T-Bili (mg/dL)	0.1 ± 0.0	0.1 ± 0.0	0.1 ± 0.0	0.1 ± 0.0	0.1 ± 0.0	0.1 ± 0.0	0.1 ± 0.0	0.1 ± 0.0
T-Chol (mg/dL)	91.8 ± 3.1	93.0 ± 3.2	94.4 ± 5.7	91.6 ± 11.3	80.2 ± 6.8	85.2 ± 3.1	81.2 ± 7.8	84.4 ± 2.6
TG (mg/dL)	81.8 ± 16.8	53.0 ± 15.0**	46.0 ± 9.0**	51.4 ± 11.2**	69.2 ± 14.9	28.0 ± 4.9**	36.8 ± 10.8**	50.4 ± 9.6*
TP (g/dL)	4.8 ± 0.1	4.9 ± 0.2	4.7 ± 0.1	4.8 ± 0.2	4.7 ± 0.1	5.0 ± 0.2	5.0 ± 0.1	5.0 ± 0.2
Alb (g/dL)	1.8 ± 0.0	1.8 ± 0.1	1.7 ± 0.0	1.7 ± 0.1	1.8 ± 0.1	1.9 ± 0.1	1.9 ± 0.1	1.8 ± 0.1
A/G ratio	0.6 ± 0.0	0.6 ± 0.0	0.6 ± 0.0	0.6 ± 0.0	0.6 ± 0.0	0.6 ± 0.0	0.6 ± 0.0	0.6 ± 0.0

**Table 3**

Histological findings for male and female mice administered KB-0118 by oral gavage for 14 days. Some findings were observed in the liver, spleen, and colon; however, all changes were minimal and not considered indicative of toxicity.

Organ	Histological finding. Treatment doses are in mg/kg bw/day			
	Males (n = 5 per group)		Females (n = 5 per group)	
	Vehicle control	KB-0118 250	Vehicle control	KB-0118 250
Liver	With in normal limits	5	5	5
	Foci, mononuclear cell infiltration, minimal	-	-	2
Kidney	With in normal limits	5	4	5
	Foci, mononuclear cell infiltration, minimal	-	1	-
Heart	With in normal limits	5	5	5
	With in normal limits	5	4	4
Spleen	Decreased cellularity, white pulp, mild	-	1	-
	Extramedullary hematopoiesis, mild; Presence of hemosiderocytes, minimal	-	-	1
Large intestine	With in normal limits	5	3	5
	Presence of hyperplastic lymphoid follicles, submucosal, minimal	-	2	-
Small intestine	With in normal limits	5	5	5

preserving colon integrity and reducing inflammation compared to the DSS-only group (Fig. 4D). Histopathological analysis further highlighted KB-0118's efficacy, as H&E-stained sections showed reduced epithelial damage and immune cell infiltration in the KB-0118-treated mice. Quantitative histological scores confirmed this protective effect, with significantly lower scores in the KB-0118 group compared to DSS-only mice (Fig. 4E and F). *In vitro* studies with DSS-treated Caco-2 cells showed a dose-dependent increase in cell viability with KB-0118, indicating its protective effect against DSS-induced epithelial damage (Fig. 4G). These results suggest that KB-0118 mitigates inflammation

and enhances epithelial integrity, supporting its potential as a therapeutic agent for colitis.

### 3.5. Therapeutic potential of KB-0118 in a chronic T cell-mediated colitis model

The therapeutic efficacy of KB-0118 for immune-mediated inflammation was assessed in a chronic colitis model induced by adoptive transfer of CD45RB<sup>high</sup> T cells, mimicking key features of Crohn's disease (Fig. 5A). CD45RB<sup>high</sup> T cells were transferred into RAG1 KO mice,

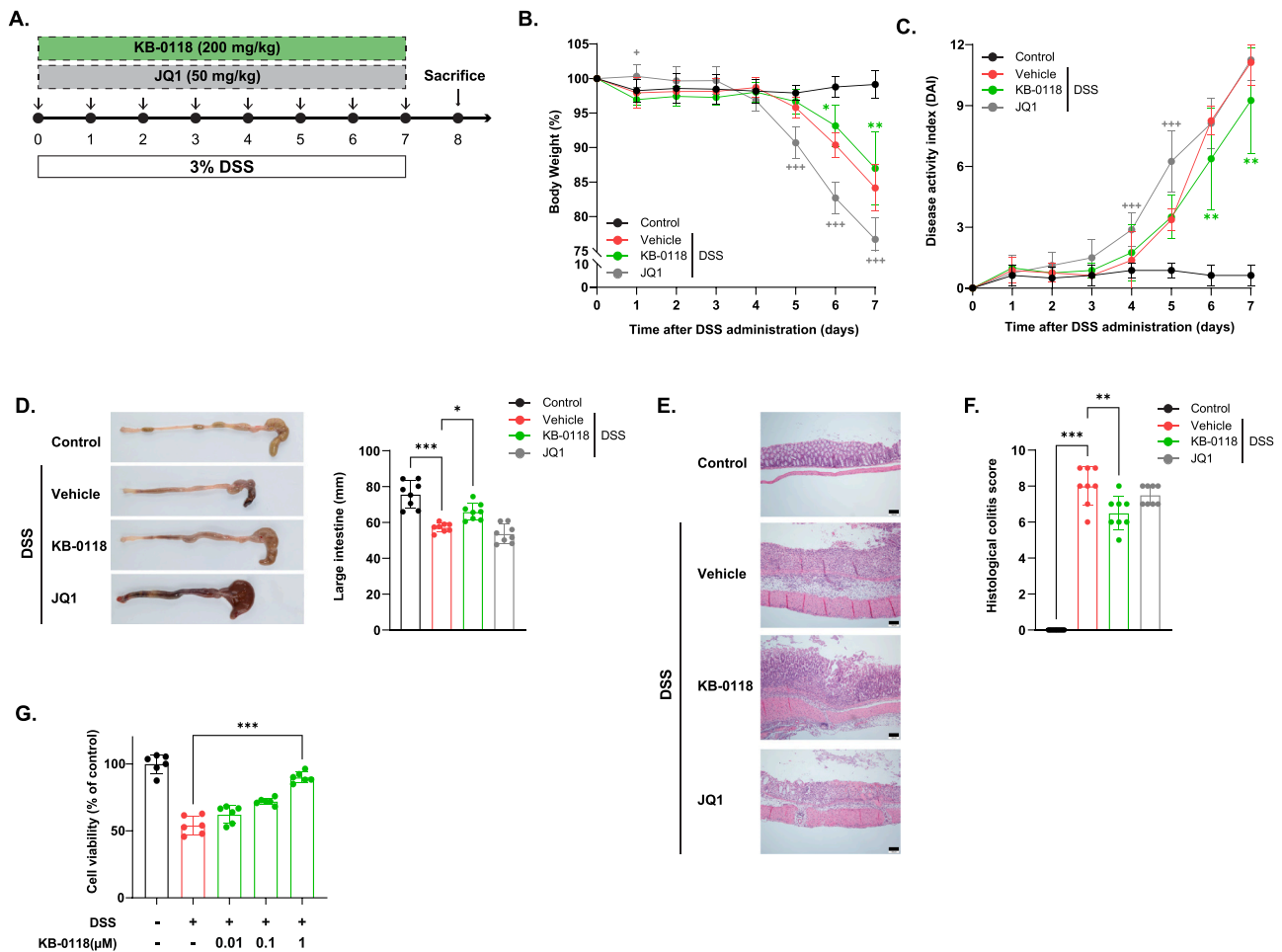


**Fig. 4.** KB-0118 mitigates DSS-induced colitis in mice. (A) Timeline of DSS and KB-0118 treatment administration. (B) Body weight progression of mice over the 7-day DSS treatment period. (C) Disease Activity Index (DAI) scores across DSS treatment groups. (D) Comparison of colon lengths in control, DSS-treated, and KB-0118-treated groups, showing reduced colon shortening with KB-0118 treatment, indicating reduced histopathological damage in KB-0118-treated mice. (E) Representative H&E-stained colon tissue sections (100x magnification), indicating reduced histopathological damage in KB-0118-treated mice. (F) Histological colitis scores highlight improved outcomes with KB-0118 treatment. (G) *In vitro* protective effects of KB-0118 on DSS-treated Caco-2 cells. Data are presented as mean  $\pm$  SD, analyzed by one-way ANOVA with Tukey's multiple comparison test. \* $p < 0.05$ ; \*\* $p < 0.01$ ; \*\*\* $p < 0.005$ ; ns, not significant.

followed by a six-week oral treatment with KB-0118 or MS402. KB-0118-treated mice showed a protective effect, with attenuated weight loss (Fig. 5B) and a trend toward increased colon length compared to vehicle-treated controls (Fig. 5C). Histopathological analysis using Hematoxylin and Eosin (H&E) staining indicated that KB-0118 reduced epithelial damage and immune cell infiltration in the colon, showing greater efficacy than MS402 (Figs. 5D and 5E). Since IL-17, a key pro-inflammatory cytokine produced by Th17 cells, is implicated in the pathology of IBD, IL-17 expression was assessed. Increased IL-17a expression was observed in the DSS-treated colons. However, treatment with KB-0118 and MS402 reduced IL-17a levels, suggesting that KB-0118 effectively modulates the Th17-mediated inflammatory response (Fig. 5D and E). These findings indicate that KB-0118 may alleviate T cell-mediated colitis by reducing IL-17a-driven inflammation, positioning it as a potential therapeutic agent for chronic IBD.

### 3.6. Transcriptomic analysis of KB-0118's immunomodulatory effects in T cell-mediated colitis

To elucidate the impact of KB-0118 on inflammation-related gene expression, transcriptomic profiles from colonic tissues in the T cell transfer colitis model were analyzed via bulk RNA sequencing. The baseline inflammatory profile, as observed in the vehicle-treated colitis group (Supplementary Figure 2), exhibited significant upregulation of

genes involved in immune activation, including *Lck*, *Stat4*, *Cd3e*, *Itgal*, and various Granzyme family members (Supplementary Figure 2A). This upregulation reflects heightened T cell activation, cytotoxicity, and immune cell migration. Gene ontology analysis highlighted enriched pathways such as "leukocyte activation," "positive regulation of immune response," and "inflammatory response" in the colitis model (Supplementary Figure 2B). Additionally, disease-related signatures associated with IBD, rheumatoid arthritis (RA), and systemic lupus erythematosus (SLE) were markedly elevated, establishing a strong inflammatory baseline typical of human inflammatory diseases (Supplementary Figure 2C). KB-0118 treatment, in contrast, demonstrated a substantial reversal of these inflammatory signatures. Heatmap analysis showed that KB-0118 significantly modulated disease-associated gene clusters, downregulating genes related to lymphocyte activation and chemotaxis (cluster 2) while upregulating genes involved in metabolic processes, including fatty acid metabolism and steroid hormone biosynthesis (cluster 3), suggesting a shift towards tissue homeostasis (Fig. 6A). Principal component analysis (PCA) further confirmed a distinct clustering of the KB-0118-treated group away from the vehicle-treated colitis group, indicating a robust transcriptomic shift induced by KB-0118 (Fig. 6B). At the gene level, KB-0118 downregulated critical genes for T cell activation and cytotoxicity, such as *Cd3e*, *Lck*, and *Stat4*, as well as integrin genes like *Itgam* and *Itgal*, suggesting reduced immune cell infiltration and inflammatory activity

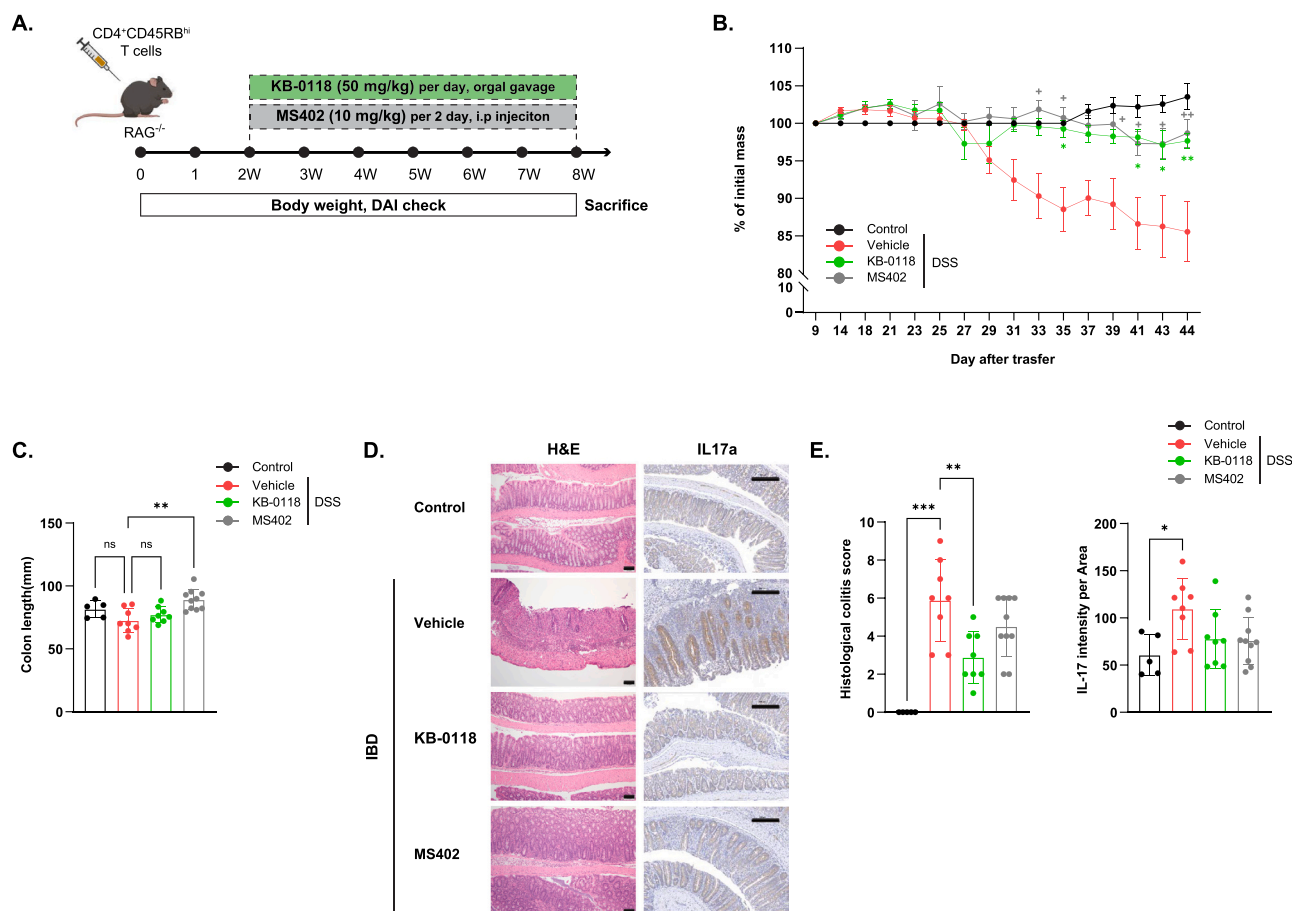


**Fig. 5.** Effect of KB-0118 on T cell transfer model of IBD in mice. (A) Timeline of T cell transfer model and KB-0118 treatment administration. (B) Body weight changes over the course of T cell transfer-induced colitis. (C) Colon length comparison among control, vehicle-treated, and KB-0118-treated groups, indicating decreased colon shortening with KB-0118. (D) Representative H&E-stained and IL-17a IHC images of colon tissues (100x magnification), showing reduced histopathological damage and IL-17a expression in the KB-0118-treated group. (E) Quantification of IL-17a positivity and histological colitis scores, demonstrating lower levels in KB-0118-treated mice compared to vehicle-treated controls. Data are presented as mean  $\pm$  SD, analyzed by two-way ANOVA with Tukey's multiple comparison test. \* $p < 0.05$ ; \*\* $p < 0.01$ ; \*\*\* $p < 0.005$ ; ns, not significant.

(Fig. 6C). Gene ontology analysis (Fig. 6D) revealed that immune-related pathways, including T cell activation and positive immune regulation, were significantly downregulated. Meanwhile, genes related to steroid and retinoid metabolism were upregulated, indicating a shift towards metabolic reprogramming. Volcano plots further highlighted the broad impact of KB-0118 on disease-associated gene signatures. In the KB-0118-treated group, 303 IBD-upregulated genes and 302 SLE-upregulated genes were significantly downregulated, while RA-related up genes also showed a notable decrease, supporting the cross-disease immunomodulatory potential of KB-0118 (Fig. 6E). Finally, regulon analysis identified transcription factors affected by KB-0118 treatment. Notably, KB-0118 downregulated target genes of BRD4 and Stat3, both of which play essential roles in Th17 differentiation and inflammatory responses, indicating an on-target effect of KB-0118 against BRD4 *in vivo*. KB-0118 also reduced expression of genes regulated by immune-related TFs, such as IRF8, FOXO1, and RUNX1, suggesting a broad suppression of inflammatory transcriptional networks (Fig. 6F). Collectively, these transcriptomic results indicate that KB-0118 effectively counteracts the inflammatory gene expression profile seen in the vehicle-treated colitis model, downregulating key immune pathways while upregulating metabolic pathways. These findings underscore KB-0118's potential as a therapeutic agent for modulating immune responses in IBD and related inflammatory diseases.

#### 4. Discussion

The therapeutic use of BET inhibitors (BETi) has shown promise across a range of diseases, from oncology to chronic inflammatory conditions such as inflammatory bowel disease (IBD). However, despite their potential, BET inhibitors are not without limitations. One major concern with existing BETi compounds, like JQ1 and I-BET762, is toxicity, which can limit their therapeutic use, particularly in chronic conditions [28]. Adverse effects related to systemic toxicity, hepatotoxicity, and myelosuppression have been reported, presenting a significant barrier to their clinical translation [29]. Furthermore, BET inhibitors often suffer from short half-lives, requiring frequent dosing, which raises concerns about patient compliance and increases the risk of cumulative toxicity [3]. These limitations underscore the need for novel BET inhibitors with improved safety profiles, enhanced potency, and extended half-lives, especially for conditions such as IBD, where long-term therapy is typically necessary [4,29].

To address these limitations, we identified KB-0118, a novel BET bromodomain inhibitor, using time-resolved fluorescence resonance energy transfer (TR-FRET) screening. This approach allowed for the selection of compounds with high specificity for BRD2 and BRD4 bromodomains, which are key regulators of immune and inflammatory responses (Fig. 1). KB-0118 showed selective binding affinity to the BD1 and BD2 domains of BRD2 and BRD4, with minimal binding to BRD3. Such selectivity suggests a reduced potential for off-target effects, thereby expanding its therapeutic window. By focusing on BRD4, a

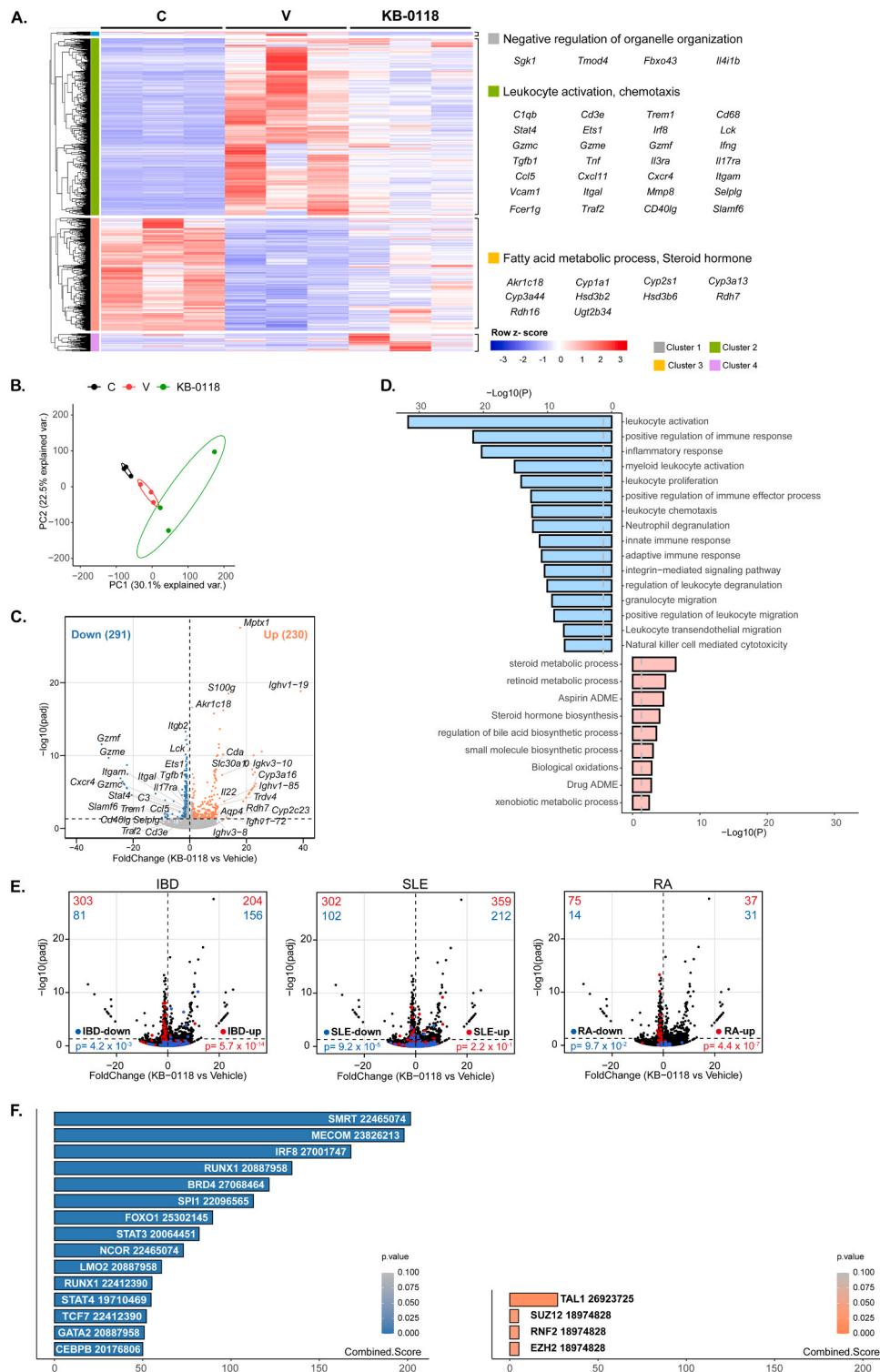


**Fig. 6.** Transcriptomic analysis of IBD model treated with KB-0118. (A) Heatmap of differentially expressed genes between control (C), IBD + vehicle (V), and IBD + KB-0118 (KB-0118) groups ( $p\text{-adj} < 0.05$ ,  $\log_2\text{FoldChange} > 1$ ), with key GO terms and genes indicated. (B) PCA plot depicting sample clustering by treatment group. (C) Volcano plot showing down- (blue) and upregulated (red) genes and (D) GO-term analysis of downregulated (blue) and upregulated (pink) gene sets in KB-0118 compared to vehicle; the gray line indicates a p-value threshold of 0.05. (E) Volcano plot superimposed with disease signature genes for IBD, SLE, and RA. (F) Transcription factor enrichment analysis in KB-0118 compared to vehicle for significantly regulated genes using ChEA 2022 data from the Enrichr tool.

central mediator of pro-inflammatory pathways, KB-0118 offers an opportunity to target inflammation more precisely while avoiding broader systemic immune suppression. Following its selection, KB-0118 underwent a thorough *in vivo* safety assessment to confirm its suitability for chronic inflammatory applications. Male and female C57BL/6 mice

treated with various doses of KB-0118 showed no significant adverse effects in body weight (Supplementary Figure 1), hematology (Table 1), blood chemistry (Table 2), or histopathology (Table 3). This favorable safety profile distinguishes KB-0118 from existing BET inhibitors, making it more suitable for chronic use in inflammatory conditions like

IBD.

KB-0118's immunomodulatory potential was validated through comprehensive *in vitro* and *in vivo* assessments. In cell-based studies, KB-0118 effectively downregulated pivotal pro-inflammatory cytokines such as *Tnf*, *Il-1 $\beta$* , and *Il-23a*, while upregulating anti-inflammatory markers like *Il-4* and *Il-10*, indicating a favorable shift in immune modulation (Fig. 2). Furthermore, KB-0118 selectively inhibited Th17 cell differentiation—a key player in IBD pathology—resulting in a notable reduction in IL-17 levels, which directly correlates with disease severity and tissue inflammation in IBD (Fig. 3). *In vivo*, KB-0118 significantly reduced disease severity in both DSS-induced (Fig. 4) and T cell-mediated (Fig. 5) colitis models by preserving colon structure, reducing histopathological damage, and attenuating IL-17 expression, demonstrating superior efficacy to standard BET inhibitors like JQ1 and MS402. These efficacy comparisons were based on key disease parameters, including disease activity index (DAI), colon length preservation, histological colitis scores, and IL-17A expression levels, as established in previous studies evaluating JQ1 in DSS-induced colitis [30] and MS402 in T cell transfer colitis [31]. Additionally, JQ1 and MS402 were administered via intraperitoneal (IP) injection due to their limited solubility, as reported in prior studies. In contrast, KB-0118, which exhibits higher solubility and intestinal absorbability, was administered via oral gavage—a more clinically relevant route for IBD treatment (Figs. 4 and 5). This distinction not only highlights KB-0118's enhanced therapeutic efficacy but also underscores its practical advantages in terms of patient compliance and ease of administration.

Given KB-0118's favorable safety profile, it may also serve as a candidate for combination therapy with existing IBD treatments. The relatively low toxicity of KB-0118 raises the possibility of synergistic or additive effects when used alongside current therapeutic agents, such as biologics (e.g., anti-TNF or IL-23 inhibitors) or small-molecule immunomodulators. Such combination approaches could enhance therapeutic efficacy while minimizing the required dosage of each drug, potentially reducing adverse effects and improving patient outcomes. Further studies will be needed to evaluate the clinical feasibility of these combination strategies.

Mechanistically, KB-0118 appears to suppress Th17-driven inflammation through epigenetic modulation of BRD4—a BET protein known to regulate gene transcription by interacting with acetylated histones (Fig. 6F). By inhibiting BRD4, KB-0118 potentially reduces chromatin accessibility at promoters of pro-inflammatory genes, curtailing Th17-related cytokine production and other inflammatory mediators. This mechanism aligns with observations in BET inhibition studies, where BRD4 suppression has been shown to modulate immune response pathways in various inflammatory conditions [29,32]. Furthermore, transcriptomic analysis of KB-0118-treated tissues revealed downregulation of STAT3 and BRD4 target genes, both crucial in Th17 differentiation and inflammatory function.

Despite these promising findings, several limitations must be considered. First, although our preclinical models provide valuable insights into the efficacy of KB-0118 in IBD, they may not fully replicate the complexity of human disease, particularly in terms of immune heterogeneity and disease progression. Differences in immune regulation between mice and humans could influence the translational applicability of our findings. Second, while KB-0118 showed a favorable safety profile in short-term studies, long-term effects, including potential off-target interactions and metabolic stability, require further investigation. Future studies should include humanized mouse models and patient-derived organoid systems to better predict the clinical relevance of KB-0118. Additionally, exploring its pharmacokinetic and pharmacodynamic properties in larger animal models will be critical for clinical translation.

Future research should focus on elucidating KB-0118's precise mechanism of action at the chromatin level, including its effects on histone acetylation and transcription factor interactions in Th17 cells. Additionally, optimization of dosing regimens through pharmacokinetic

and pharmacodynamic studies will be essential for maximizing therapeutic efficacy while minimizing potential side effects. Another key area for future investigation is the identification of predictive biomarkers that could enable patient stratification in clinical trials, ensuring that KB-0118 is administered to patients most likely to benefit from its immunomodulatory effects. Ultimately, these studies will be critical for advancing KB-0118 toward clinical translation as a promising therapeutic for IBD and other inflammatory diseases.

In conclusion, this study introduces KB-0118 as a potent BET bromodomain inhibitor with significant efficacy in modulating immune responses in IBD models. Through its selective inhibition of Th17 differentiation and targeted anti-inflammatory actions, KB-0118 demonstrates potential as a safer, more effective therapeutic alternative for chronic inflammatory diseases. Additionally, the possibility of combination therapy with existing IBD treatments provides a promising avenue for future research, particularly in enhancing treatment efficacy while reducing adverse effects. While KB-0118 represents a promising candidate, further investigations into its long-term safety and translational potential are necessary before advancing to clinical trials. Continued research into KB-0118's mechanisms and therapeutic applications, particularly in optimizing dosing, identifying biomarkers, and validating human-specific responses, will be critical for its successful clinical development.

## Funding

This research was supported by grants from the Ministry of SMEs and Startups (RS-2022-TI022458), from the Ministry of Health & Welfare, Republic of Korea (RS-2024-00438443), and Basic Science Research Program through the National Research Foundation of Korea (NRF) funded by the Ministry of Education (2021R111A1A0106036912, RS-2024-00462081, 2019R1A6A1A03032869).

## CRedit authorship contribution statement

**Kim Gi-Cheon:** Writing – original draft, Supervision, Resources, Project administration, Investigation, Conceptualization. **Lee In-hyun:** Writing – original draft, Validation, Resources, Investigation, Formal analysis, Conceptualization. **Jeong Yeo-Jin:** Writing – original draft, Validation, Methodology, Investigation, Formal analysis, Conceptualization. **Kwon Ho-Keun:** Writing – original draft, Supervision, Resources, Project administration, Investigation, Funding acquisition, Conceptualization. **Kwon Gi-Nam:** Formal analysis. **Ok Yeon-Su:** Formal analysis. **Chun Jin Hong:** Validation. **Kim Min-Young:** Writing – original draft, Validation, Formal analysis. **Yang Haemi:** Validation, Formal analysis. **Kang Sukmo:** Validation, Formal analysis, Conceptualization. **Son Minhee:** Validation, Formal analysis.

## Declaration of Generative AI and AI-assisted technologies in the writing process

The manuscript was edited for English language accuracy using the Grammarly program.

## Declaration of Competing Interest

The authors declare that they have no known competing financial interests or personal relationships that could have appeared to influence the work reported in this paper.

## Acknowledgments

The graphical abstract was created using BioRender.com.

## Appendix A. Supporting information

Supplementary data associated with this article can be found in the online version at [doi:10.1016/j.biopha.2025.117933](https://doi.org/10.1016/j.biopha.2025.117933).

## Data availability

The data that has been used is confidential.

## References

- [1] P. Filippakopoulos, J. Qi, S. Picaud, Y. Shen, W.B. Smith, O. Fedorov, E.M. Morse, T. Keates, T.T. Hickman, I. Felletar, M. Philpott, S. Munro, M.R. McKeown, Y. Wang, A.L. Christie, N. West, M.J. Cameron, B. Schwartz, T.D. Heighman, N. La Thangue, C.A. French, O. Wiest, A.L. Kung, S. Knapp, J.E. Bradner, Selective inhibition of BET bromodomains, *Nature* 468 (7327) (2010) 1067–1073.
- [2] B. Donati, E. Lorenzini, A. Ciarrocchi, BRD4 and cancer: going beyond transcriptional regulation, *Mol. Cancer* 17 (1) (2018) 164.
- [3] J.E. Delmore, G.C. Issa, M.E. Lemieux, P.B. Rahl, J. Shi, H.M. Jacobs, E. Kastiritis, T. Gilpatrick, R.M. Paranal, J. Qi, M. Chesi, A.C. Schinzel, M.R. McKeown, T. P. Heffernan, C.R. Vakoc, P.L. Bergsagel, I.M. Ghobrial, P.G. Richardson, R. A. Young, W.C. Hahn, K.C. Anderson, A.L. Kung, J.E. Bradner, C.S. Mitsiades, BET bromodomain inhibition as a therapeutic strategy to target c-Myc, *Cell* 146 (6) (2011) 904–917.
- [4] M. Muhar, A. Ebert, T. Neumann, C. Umkehrer, J. Jude, C. Wieshofer, P. Rescheneder, J.J. Lipp, V.A. Herzog, B. Reichholz, D.A. Cisneros, T. Hoffmann, M.F. Schlapansky, P. Bhat, A. von Haeseler, T. Köcher, A.C. Obenauf, J. Popow, S. L. Ameres, J. Zuber, SLAM-seq defines direct gene-regulatory functions of the BRD4-MYC axis, *Science* 360 (6390) (2018) 800–805.
- [5] J. Zuber, J. Shi, E. Wang, A.R. Rappaport, H. Herrmann, E.A. Sison, D. Magoon, J. Qi, K. Blatt, M. Wunderlich, M.J. Taylor, C. Johns, A. Chicas, J.C. Mulloy, S. C. Kogan, P. Brown, P. Valent, J.E. Bradner, S.W. Lowe, C.R. Vakoc, RNAi screen identifies Brd4 as a therapeutic target in acute myeloid leukaemia, *Nature* 478 (7370) (2011) 524–528.
- [6] S.R. Floyd, M.E. Pacold, Q. Huang, S.M. Clarke, F.C. Lam, I.G. Cannell, B.D. Bryson, J. Rameseder, M.J. Lee, E.J. Blake, A. Fydrich, R. Ho, B.A. Greenberger, G.C. Chen, A. Maffa, A.M. Del Rosario, D.E. Root, A.E. Carpenter, W.C. Hahn, D.M. Sabatini, C. C. Chen, F.M. White, J.E. Bradner, M.B. Yaffe, The bromodomain protein Brd4 insulates chromatin from DNA damage signalling, *Nature* 498 (7453) (2013) 246–250.
- [7] K. Klein, Bromodomain protein inhibition: a novel therapeutic strategy in rheumatic diseases, *RMD Open* 4 (2) (2018) e000744.
- [8] M. Mann, Y. Fu, X. Xu, D.S. Roberts, Y. Li, J. Zhou, Y. Ge, A.R. Brasier, Bromodomain-containing protein 4 regulates innate inflammation in airway epithelial cells via modulation of alternative splicing, *bioRxiv* (2023).
- [9] J. Shi, C.R. Vakoc, The mechanisms behind the therapeutic activity of BET bromodomain inhibition, *Mol. Cell* 54 (5) (2014) 728–736.
- [10] E. Nicodeme, K.L. Jeffrey, U. Schaefer, S. Beinke, S. Dewell, C.W. Chung, R. Chandwani, I. Marazzi, P. Wilson, H. Coste, J. White, J. Kirilovsky, C.M. Rice, J. M. Lora, R.K. Prinjha, K. Lee, A. Tarakhovskiy, Suppression of inflammation by a synthetic histone mimic, *Nature* 468 (7327) (2010) 1119–1123.
- [11] D.A. Mele, A. Salmeron, S. Ghosh, H.R. Huang, B.M. Bryant, J.M. Lora, BET bromodomain inhibition suppresses TH17-mediated pathology, *J. Exp. Med.* 210 (11) (2013) 2181–2190.
- [12] D.B. Graham, R.J. Xavier, Pathway paradigms revealed from the genetics of inflammatory bowel disease, *Nature* 578 (7796) (2020) 527–539.
- [13] H. Bugaut, S. Aractingi, Major role of the IL17/23 axis in psoriasis supports the development of new targeted therapies, *Front. Immunol.* 12 (2021) 621956.
- [14] L. Rovedatti, T. Kudo, P. Biancheri, M. Sarra, C.H. Knowles, D.S. Rampton, G. R. Corazza, G. Monteleone, A. Di Sabatino, T.T. Macdonald, Differential regulation of interleukin 17 and interferon gamma production in inflammatory bowel disease, *Gut* 58 (12) (2009) 1629–1636.
- [15] K. Cheung, G. Lu, R. Sharma, A. Vincek, R. Zhang, A.N. Plotnikov, F. Zhang, Q. Zhang, Y. Ju, Y. Hu, L. Zhao, X. Han, J. Meslamani, F. Xu, A. Jaganathan, T. Shen, H. Zhu, E. Rusinova, L. Zeng, J. Zhou, J. Yang, L. Peng, M. Ohlmeyer, M. J. Walsh, D.Y. Zhang, H. Xiong, M.M. Zhou, BET N-terminal bromodomain inhibition selectively blocks Th17 cell differentiation and ameliorates colitis in mice, *Proc. Natl. Acad. Sci. USA* 114 (11) (2017) 2952–2957.
- [16] S. Ghosh, J.M. Lora, Suppression of TH17-mediated pathology through BET bromodomain inhibition, *Drug Discov. Today.: Technol.* 19 (2016) 39–44.
- [17] J. Niu, Y. Guo, G. Jing, H. Wang, L. Yang, Y. Li, Y. Gao, H. Wang, A. Li, X. Xu, Y. Qian, J. Fei, S. Wang, Anion-dependent layered double hydroxide nanoparticles regulate differentiation of CD206+ CX3CR1+ macrophages by inhibiting the IL-17 signaling pathway contributing to inflammatory bowel disease, *Adv. Funct. Mater.* 34 (14) (2024) 2305042.
- [18] J. Zhao, Q. Lu, Y. Liu, Z. Shi, L. Hu, Z. Zeng, Y. Tu, Z. Xiao, Q. Xu, Th17 Cells in inflammatory bowel disease: cytokines, plasticity, and therapies, *J. Immunol. Res.* 2021 (1) (2021) 8816041.
- [19] A. Ueno, L. Jeffery, T. Kobayashi, T. Hibi, S. Ghosh, H. Jijon, Th17 plasticity and its relevance to inflammatory bowel disease, *J. Autoimmun.* 87 (2018) 38–49.
- [20] A.M. Bolger, M. Lohse, B. Usadel, Trimmomatic: a flexible trimmer for Illumina sequence data, *Bioinformatics* 30 (15) (2014) 2114–2120.
- [21] D. Kim, B. Langmead, S.L. Salzberg, HISAT: a fast spliced aligner with low memory requirements, *Nat. Methods* 12 (4) (2015) 357–360.
- [22] M. Pertea, G.M. Pertea, C.M. Antonescu, T.-C. Chang, J.T. Mendell, S.L. Salzberg, StringTie enables improved reconstruction of a transcriptome from RNA-seq reads, *Nat. Biotechnol.* 33 (3) (2015) 290–295.
- [23] L. Massimino, L.A. Lamparelli, Y. Houshyar, S. D'Alessio, L. Peyrin-Biroulet, S. Vetrano, S. Danese, F. Ungaro, The inflammatory bowel disease transcriptome and metatranscriptome meta-analysis (IBD TaMMA) framework, *Nat. Comput. Sci.* 1 (8) (2021) 511–515.
- [24] D. Nehar-Belaid, S. Hong, R. Marches, G. Chen, M. Bolisetty, J. Baisch, L. Walters, M. Punaro, R.J. Rossi, C.H. Chung, R.P. Huynh, P. Singh, W.F. Flynn, J.A. Tabanor-Gayle, N. Kuchipudi, A. Mejias, M.A. Collet, A.L. Lucido, K. Palucka, P. Robson, S. Lakshminarayanan, O. Ramilo, T. Wright, V. Pascual, J.F. Banchereau, Mapping systemic lupus erythematosus heterogeneity at the single-cell level, *Nat. Immunol.* 21 (9) (2020) 1094–1106.
- [25] Y. Ao, Z. Wang, J. Hu, M. Yao, W. Zhang, Identification of essential genes and immune cell infiltration in rheumatoid arthritis by bioinformatics analysis, *Sci. Rep.* 13 (1) (2023) 2032.
- [26] A. Bénard, A. Mittelstädt, B. Klösch, K. Glanz, J. Müller, J. Schoen, B. Nüse, M. Brunner, E. Naschberger, M. Stürzl, J. Mattner, L.E. Muñoz, K. Sohn, R. Grützmann, G.F. Weber, IL-3 orchestrates ulcerative colitis pathogenesis by controlling the development and the recruitment of splenic reservoir neutrophils, *Cell Rep.* 42 (6) (2023).
- [27] J. Saravia, N.M. Chapman, H. Chi, Helper T cell differentiation, *Cell. Mol. Immunol.* 16 (7) (2019) 634–643.
- [28] D.B. Doroshow, J.P. Eder, P.M. LoRusso, BET inhibitors: a novel epigenetic approach, *Ann. Oncol.* 28 (8) (2017) 1776–1787.
- [29] Z.-Q. Wang, Z.-C. Zhang, Y.-Y. Wu, Y.-N. Pi, S.-H. Lou, T.-B. Liu, G. Lou, C. Yang, Bromodomain and extraterminal (BET) proteins: biological functions, diseases and targeted therapy, *Signal Transduct. Target. Ther.* 8 (1) (2023) 420.
- [30] H. Lee, J. Nam, H. Jang, Y.S. Park, M.H. Son, I.H. Lee, S.I. Eyun, J.H. Yang, J. Jeon, S. Yang, BRD2-specific inhibitor, BBC0403, inhibits the progression of osteoarthritis pathogenesis in osteoarthritis-induced C57BL/6 male mice, *Br. J. Pharmacol.* 181 (15) (2024) 2528–2544.
- [31] H. Lee, J. Nam, H. Jang, Y.S. Park, M.H. Son, I.H. Lee, S.I. Eyun, J. Jeon, S. Yang, Novel molecule BBC0901 inhibits BRD4 and acts as a catabolic regulator in the pathogenesis of osteoarthritis, *Biomed. Pharmacother.* 166 (2023) 115426.
- [32] N. Wang, R. Wu, D. Tang, R. Kang, The BET family in immunity and disease, *Signal Transduct. Target. Ther.* 6 (1) (2021) 23.